

# Airflow visualization in a model of human glottis near the self-oscillating vocal folds model

J. Horáček<sup>a,\*</sup>, V. Uruba<sup>a</sup>, V. Radolf<sup>a</sup>, J. Veselý<sup>a</sup>, V. Bula<sup>a</sup>

<sup>a</sup>*Institute of Thermomechanics, Academy of Sciences of the Czech Republic*

Received 1 October 2010; received in revised form 10 March 2011

---

## Abstract

The contribution describes PIV (Particle Image Velocimetry) measurement of airflow in the glottal region of complex physical models of the voice production that consist of 1 : 1 scaled models of the trachea, the self-oscillating vocal folds and the human vocal tract with acoustical spaces that correspond to the vowels /a:/, /u:/ and /i:/. The time-resolved PIV method was used for visualization of the airflow simultaneously with measurements of subglottal pressure, radiated acoustic pressure and vocal fold vibrations. The measurements were performed within a physiologically real range of mean airflow rate and fundamental phonation frequency. The images of the vibrating vocal folds during one oscillation period were recorded by the high-speed camera at the same time instants as the velocity fields measured by the PIV method.

In the region above the models of the ventricular folds and of the epilaryngeal tube it is possible to detect large vortices with dimensions comparable with the channel cross-section and moving relatively slowly downstream. The vortices disappear in the narrower pharyngeal part of the vocal tract model where the flow is getting more uniform. The basic features of the coherent structures identified in the laryngeal cavity models in the interval of the measured airflow rates were found qualitatively similar for all three vowels investigated.

© 2011 University of West Bohemia. All rights reserved.

*Keywords:* biomechanics of human voice, voice production modelling, PIV measurement of streamline patterns

---

## 1. Introduction

Physical theoretical background of the human voice production is the so-called source-filter theory [6]. The airflow coming from the lungs induces the vocal-folds self-oscillations generating a primary laryngeal acoustic signal. The acoustic resonances in the human vocal tract modify the spectrum of the primary laryngeal tone according to the vocal tract cavity shape typical for each vowel or voiced consonant. However, an exact physical mechanism changing the airflow energy into the acoustic energy in the glottis is not yet properly known. Because the investigation of the airflow pattern in the glottis region in vivo is problematic, the measurements of the flow characteristics and regimes are provided on various physical models.

Sophisticated experiments were recently performed by Neubauer et. al [3] studying the coherent structures in a free air jet near self-oscillating vocal folds. Influence of a vocal folds asymmetry on skewing of the glottal free jet was studied by Pickup & Thomson [4] using self-oscillating vocal folds made of two-layer silicon rubber modelling the vocal fold body and cover. Becker et. al [1] modelled a full fluid-structure-acoustic interaction in a test rig using self-oscillating polyurethane model of the vocal folds and taking into account influence of a simplified vocal tract model on the air jet focusing on Coanda effect.

---

\*Corresponding author. Tel.: +420 266 053 125, e-mail: jaromirh@it.cas.cz.

The present contribution describes a complex physical models of the voice production that consist of simplified 1 : 1 scaled models of the trachea, the self-oscillating vocal folds and the vocal tract with acoustical spaces that correspond to the vowels /a:/, /u:/ and /i:/. The time-resolved PIV (Particle Image Velocimetry) method was used for visualization of the airflow inside the vocal tract models simultaneously with measurements of subglottal pressure, radiated acoustic pressure and vocal fold vibrations.

## 2. Measurement set-up

The schema of the measurement set-up is shown in Fig. 1. Prior to the measurement, the storage tank was filled by the tracing particles using the cigarette smoke. The airflow was coming from a big pressure vessel and the mean airflow rate was controlled by the digital flow controller AALBORG DFC4600 and measured by the float flowmeter.

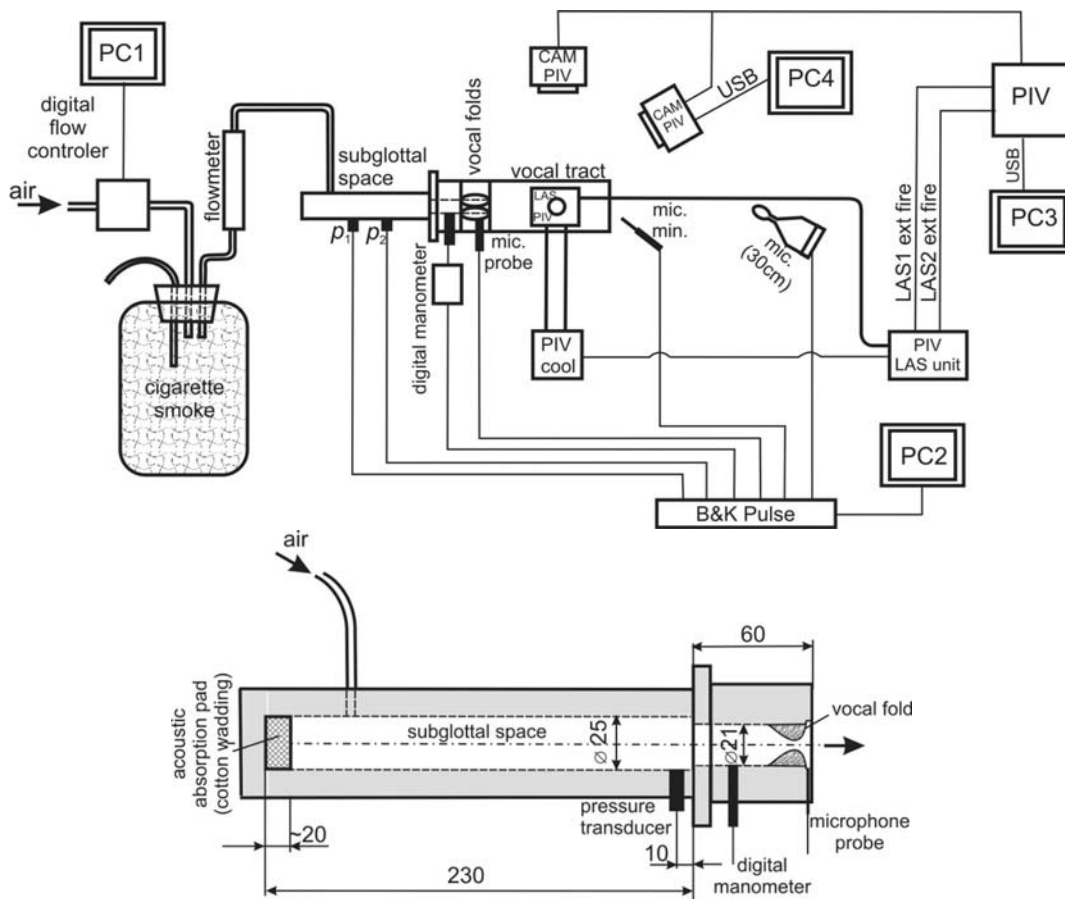


Fig. 1. Schematic simplified measurement set-up and a detail of the subglottal and glottal part

The subglottal pressure in the trachea, modeled by a Plexiglas tube, was measured by the dynamic semiconductor pressure transducers IT AS CR and the mean value by the digital manometer Greisinger Electronic GDH07AN. The vocal folds model, joined to the model of the subglottal spaces, was fabricated from a latex thin cover filled by a very soft polyurethane rubber prepared from VytaFlex 10 (parts A and B and softener So-Flex mixed in the ratio: 1 : 1 : 3). The Plexiglas “2D” vocal tract models developed from acoustically equivalent 3D FE models [7] are shown in Fig. 2. The double laser light sheet generated by the PIV system DAN-TEC was focused on a part of the vocal tract model observed by the PIV high-speed camera.

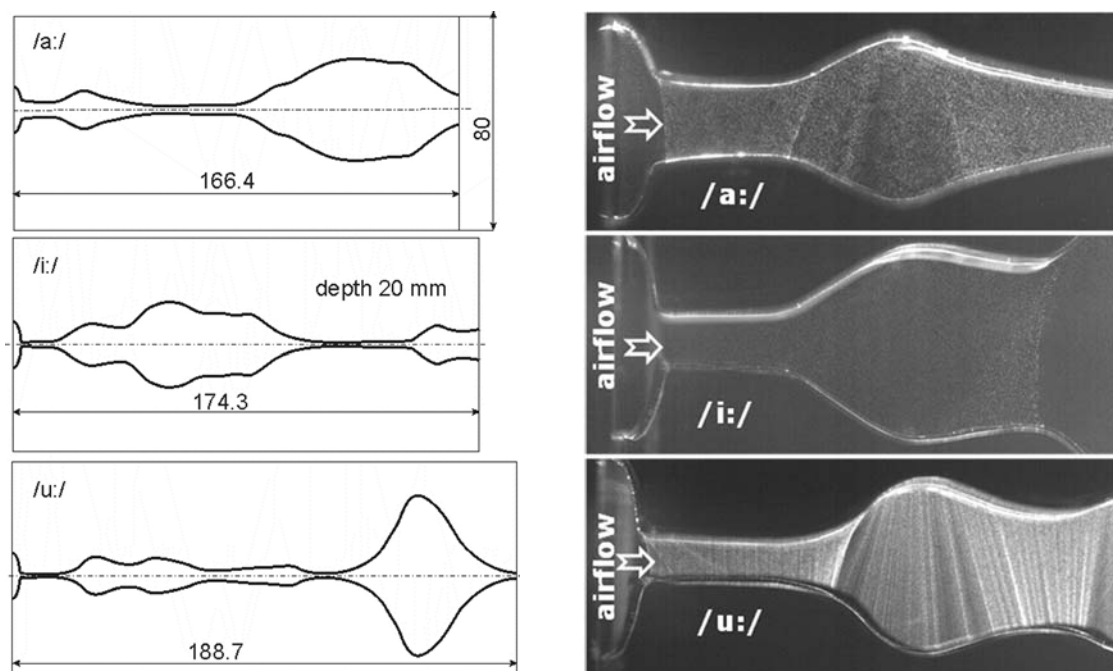


Fig. 2. Models of the human vocal tract for vowels /a:/, /i:/ and /u:/ (left) and field of view of the glottal region with flowing particles in the PIV laser light (right)

The self-oscillating vocal folds were synchronously recorded by the second high-speed camera NANONSENSE Mk III, Nikon at the same time instants as the velocity fields measured by the PIV method. The generated acoustic signal was monitored by the miniature 1/8” pressure field microphone B&K 4138 at the mouth and by the sound level meter B&K 2239 in the distance 30 cm from the outlet of the vocal tract model. The time signals from the pressure transducers and microphones were measured by the B&K system PULSE 10 with the Controller Module MPE 7537A and controlled by a personal computer. Another computer was used for recording the vocal folds vibrations by the high-speed camera at the same instants as the velocity fields measured by the PIV method. PIV laser frequency was 1 kHz and 2 000 snapshots were recorded.

The measurements were performed within a physiologically real range of input parameters for the mean airflow rate ( $Q_{\text{mean}} = 0.2 - 0.6$  l/s), the mean subglottal pressure ( $P_{\text{sub}} = 0.9 - 2.1$  kPa) and the fundamental frequency ( $F_0 = 140 - 192$  Hz) — see tab 1.

Table 1. Basic measurement data and settings

vowel	mean flow rate	subglottal pressure			microphone signal (at the “lips”)	fundamental frequency	PIV laser double pulse delay
	$Q$ [l/s]	$P_{\text{sub}}$ [Pa]	RMS [Pa]	SPL [dB]	SPL [dB]	$F_0$ [Hz]	$\Delta t$ [ $\mu\text{s}$ ]
/a:/	0.23	990	989	133	98.1	180	40
/i:/	0.21	940	974	138	95.4	148	30
/u:/	0.21	930	888	131	107	192	30

### 3. Results

The glottal gap width evaluated from the series of the images of the vibrating vocal folds in the cross-section plane, where the flow visualization by PIV was performed, are in Fig. 3 and the measured subglottal pressure and spectra of the microphone signals are shown in Fig. 4.

The signals are not perfectly periodic, because the vocal fold vibrations were not exactly repeatable in each oscillation cycle and the sampling frequency of the high-speed camera was not sufficient due to the limits of the frequency range of the PIV system. The fundamental frequency  $F_0$  (see Table 1) dominates in all signals. The acoustic signals contain essential higher harmonics in the lower frequency region and clearly visible resonant frequencies in higher frequency

Table 2. Calculated formant frequencies of the “2D” vocal tracts for vowels /a:/, /u:/ and /i:/ (input parameters: speed of sound 343 m/s, air density 1.2 kg/m<sup>3</sup>, with radiation losses and boundary conditions: a) C–O ... closed at the vocal folds – open at the mouth, b) O–O ... open at the vocal folds – open at the mouth)

vowel		$F_1$ [Hz]	$F_2$ [Hz]	$F_3$ [Hz]	$F_4$ [Hz]	$F_5$ [Hz]
/a:/	C–O	572	987	2 863	3 557	4 321
	O–O	897	1 805	2 985	3 920	5 254
/i:/	C–O	246	2 182	2 620	3 266	4 205
	O–O	516	2 475	2 728	3 958	4 629
/u:/	C–O	386	739	2 044	2 618	4 035
	O–O	561	864	2 224	3 926	4 982

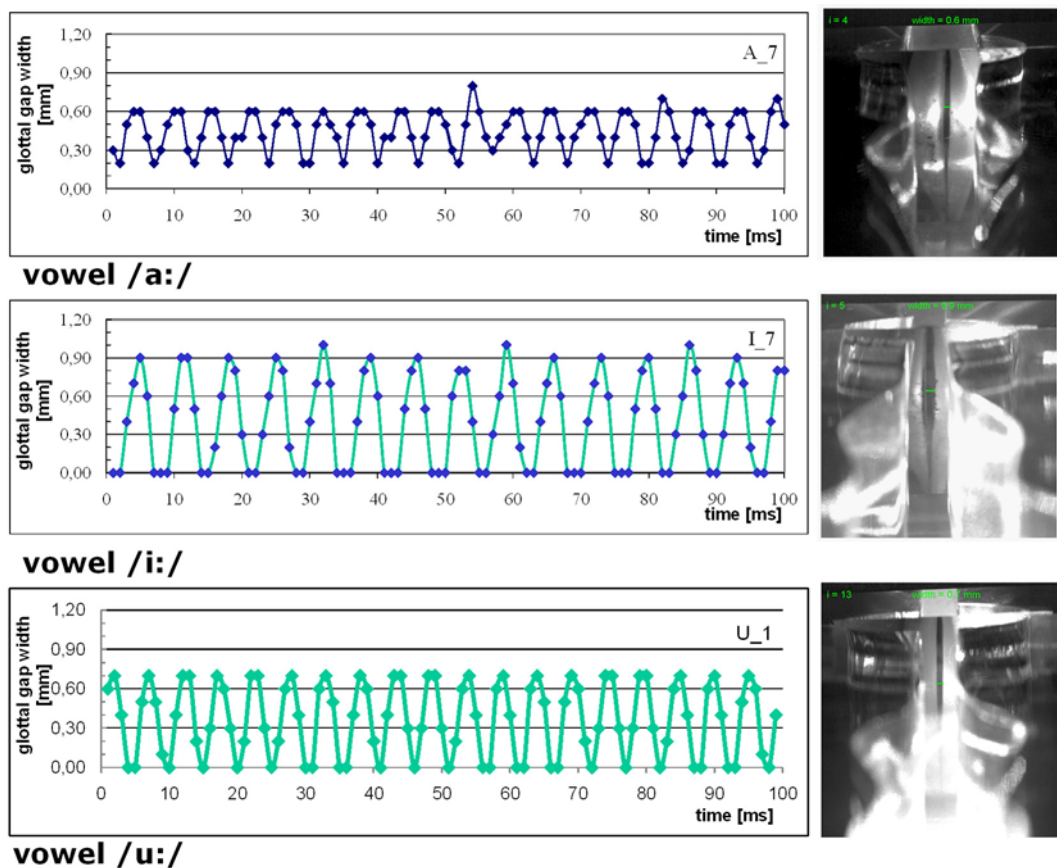


Fig. 3. Measured glottal gap in time domain (left) evaluated for all vowels at each time instant from the images of the self-oscillating vocal folds (right)

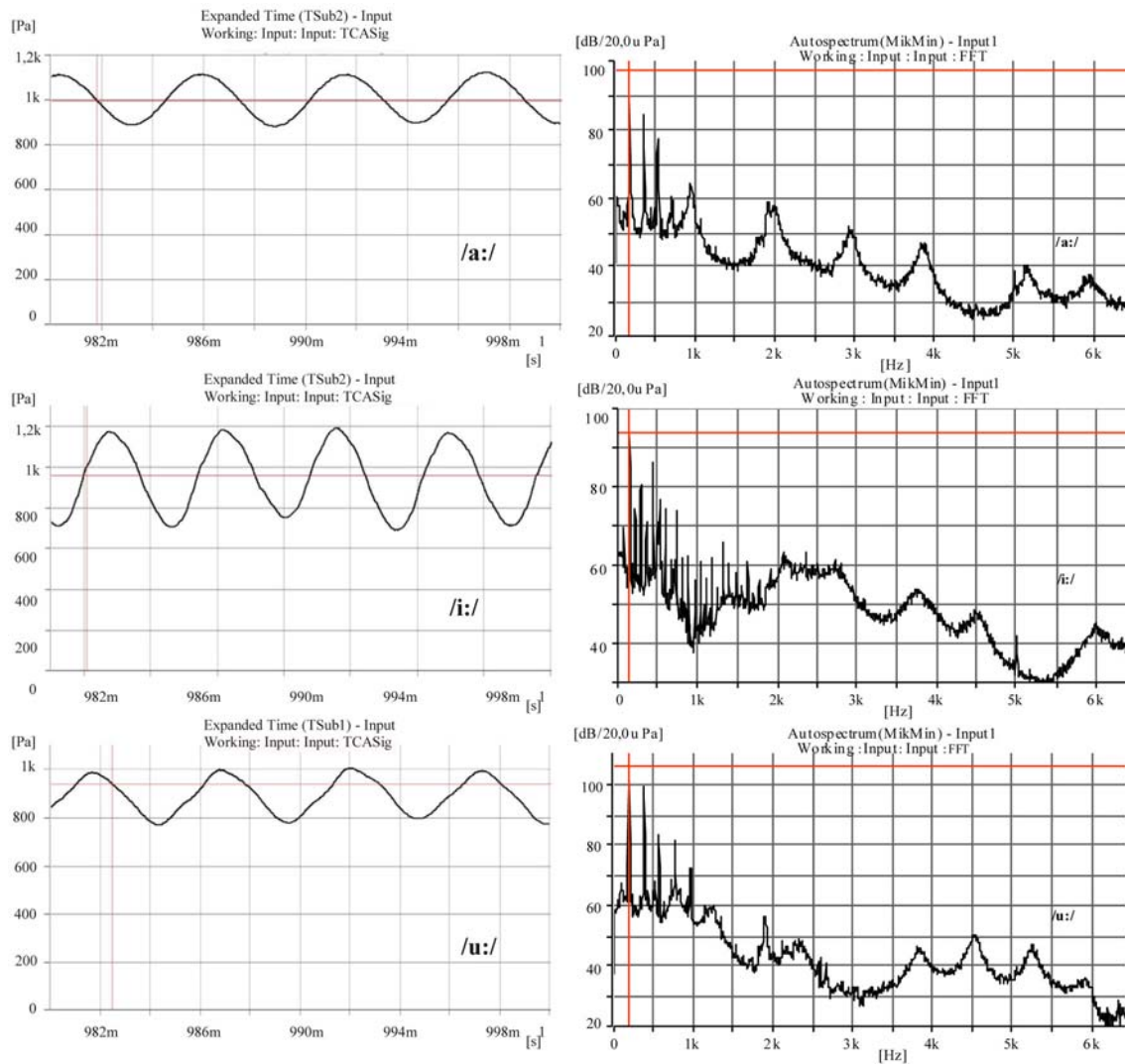


Fig. 4. Measured subglottal pressure for vowels /a:/, /i:/ and /u:/ (left) and spectra of the microphone signal at the mouth models (right)

region (see Fig. 4). The formant frequencies, e.g. for the vowel /a:/ at about  $F_1 \cong 900$  Hz,  $F_2 \cong 1.9$  kHz,  $F_3 \cong 3$  kHz and  $F_4 \cong 3.9$  kHz detected in the microphone spectrum approximately agree with the computed formant frequencies for open-open boundary conditions in Table 1, similar correspondence between calculated and measured formants is detected for the vowel /i:/, however some other parasitic resonant frequencies of an unknown origin can be seen in the spectrum for vowel /u:/, e.g. near 1.2 kHz.

The airflow streamline patterns evaluated from the PIV measurement in the laryngeal and epiglottis part of the vocal tract model for vowels /a:/, /u:/ and /i:/ are shown in Figs. 5–7. The denoted images ( $i = 1, 2, \dots, 10$ ) and the time instants exactly correspond to the sampling frequency of the glottal gap width as shown in Fig. 3. The images  $i = 1 - 10$  of the vibrating vocal folds recorded at the same time instants are added to the left hand side of each streamline pattern. A small circle on each image denotes the position of a point with the maximum value of the airflow velocity evaluated at each time instant. The maximum airflow velocities up to about 10 m/s were observed in the epilaryngeal tube of the model. The flow is asymmetric; the jet is skewed and attached to the upper or lower wall of the channel resembling the Coanda effect. Large eddies with dimensions comparable with the channel cross-section can be identified in a

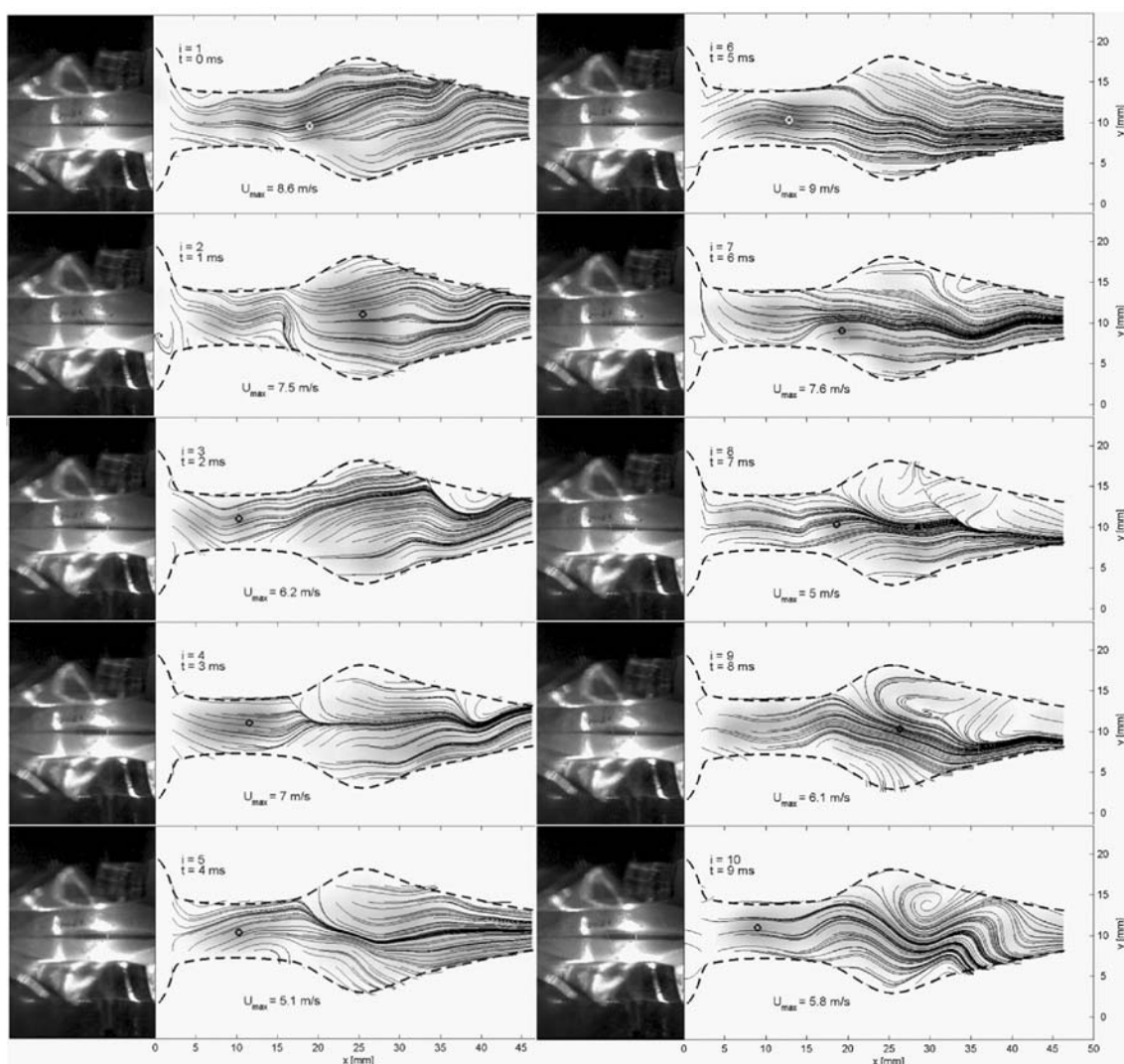


Fig. 5. Airflow streamlines measured in the model of the glottal region for vowel /a:/ and the snapshots of the self-oscillating vocal folds (left part of the panels) registered at the time instants corresponding to the time steps  $i = 1 - 10$  in Fig. 3. The air flows from left to right. ( $Q_{\text{mean}} = 0.21$  l/s,  $P_{\text{sub}} = 940$  Pa,  $F_0 = 180$  Hz)

wider region above the laryngeal vestibule (ventricular folds and epilaryngeal tube) model. The vortices disappear in the narrower pharyngeal part of the vocal tract model where the flow is getting more uniform. The basic features of the coherent structures identified in the laryngeal cavity models in the interval of the measured airflow rates were found qualitatively similar for all three vowels investigated.

#### 4. Conclusions

The results show the following tendencies:

- the airflow streamline patterns measured in the models of the vocal tract for vowels /a:/, /u:/ and /i:/ showed large eddies with dimensions comparable with the channel cross-section detected in a wider region above the ventricular folds in the laryngeal cavity,
- the vortices generated by the pulsating jet behind the self-oscillating vocal folds, nearly periodically closing the channel, disappear in the narrower pharyngeal part of the vocal tract model where the flow accelerates and is getting more uniform,

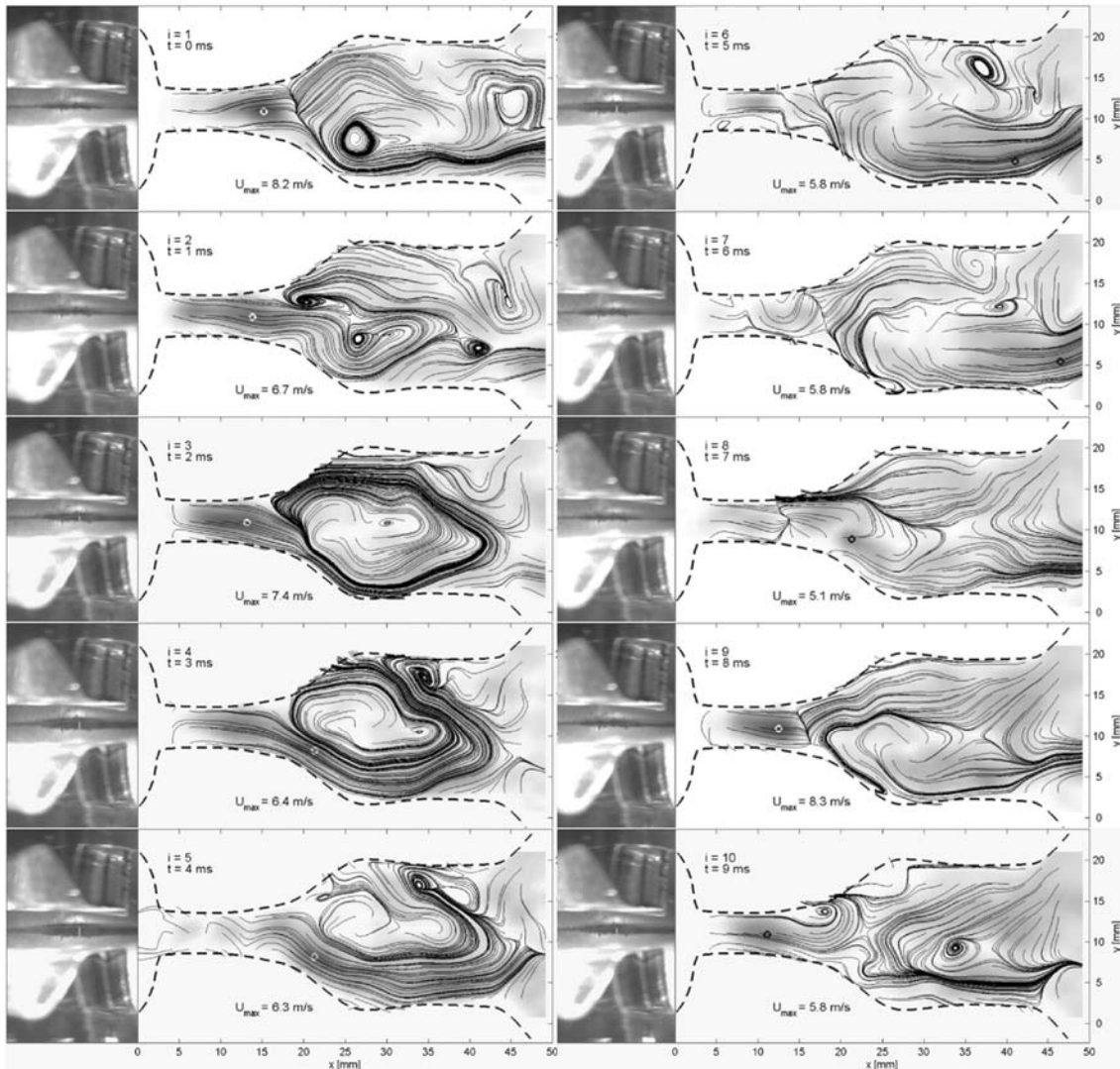


Fig. 6. Airflow streamlines measured in the model of the glottal region for vowel /i:/ and the snapshots of the self-oscillating vocal folds (left part of the panels) registered at the time instants corresponding to the time steps  $i = 1 - 10$  in Fig. 3. The air flows from left to right. ( $Q_{\text{mean}} = 0.24$  l/s,  $P_{\text{sub}} = 910$  Pa,  $F_0 = 148$  Hz)

- the basic features of the coherent structures identified in the laryngeal cavity models in the interval of the measured air flow rates were qualitatively similar for all three vowels investigated,
- substantial 3D effects were observed in the PIV experiments, see e.g. some nodes (cf. [2]) in the flow topology for  $t = 0$  and 8 ms in Fig. 6 at the end of the epilaryngeal tube model.

The experimental results are important for checking the simultaneously developed numerical models of phonation, where similar coherent structures in the glottis are numerically simulated [5].

### Acknowledgements

The research is supported by the project GACR 101/08/1155.

### References

- [1] Becker, S., Kniesburges, S., Müller, S., Delgado, A., Link, G., Kaltenbacher, M., Döllinger, M., Flow-structure-acoustic interaction in human voice model, *Journal of Acoustical Society of America*, 125 (2009) 1 351–1 361.

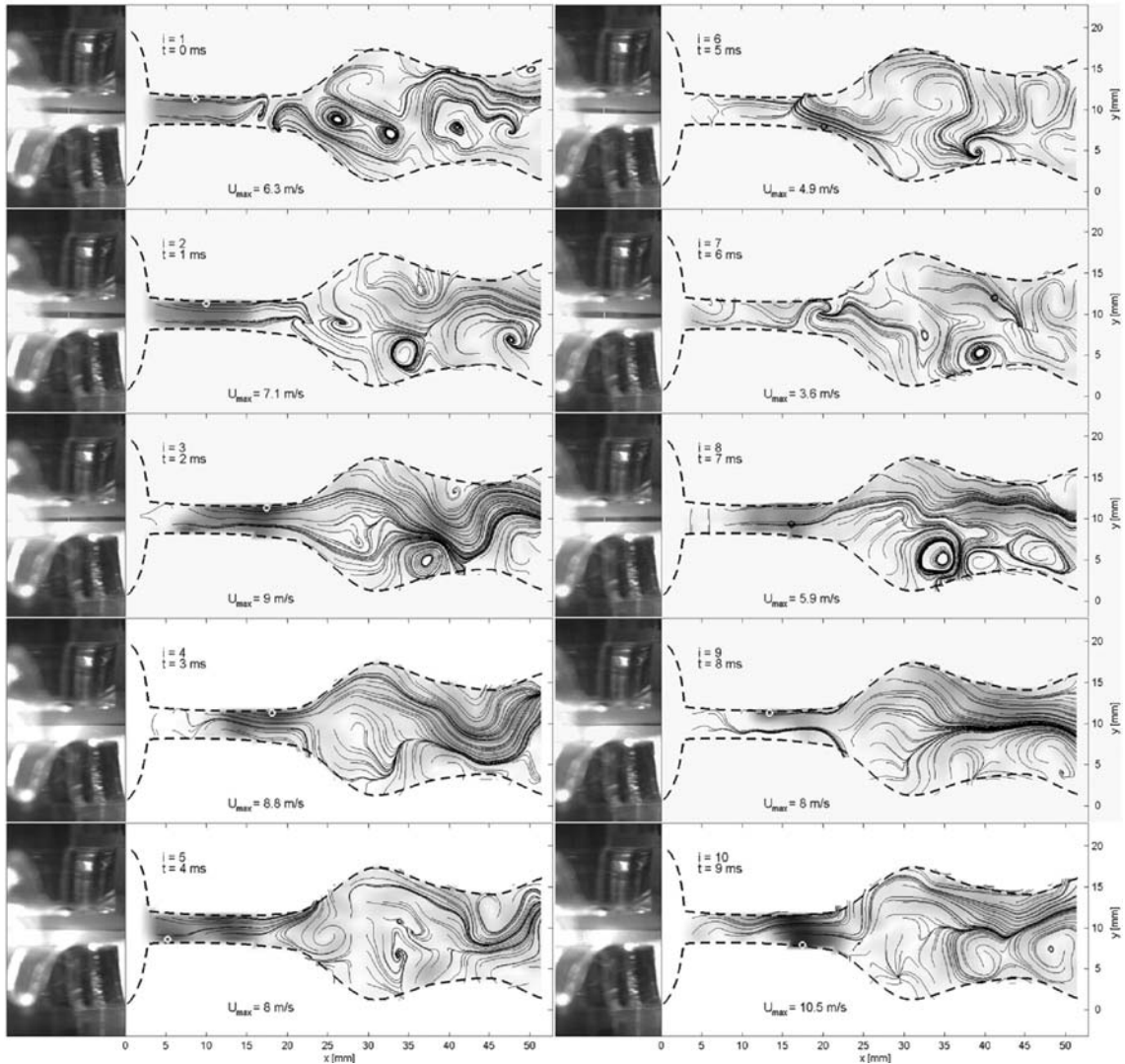


Fig. 7. Airflow streamlines measured in the model of the glottal region for vowel /u:/ and the snapshots of the self-oscillating vocal folds (left part of the panels) registered at the time instants corresponding to the time steps  $i = 1 - 10$  in Fig. 3. The air flows from left to right. ( $Q_{\text{mean}} = 0.21$  l/s,  $P_{\text{sub}} = 930$  Pa and  $F_0 = 192$  Hz)

- [2] Jacobs, G. B., Surana, A., Peacock, T., Haller, G., Identification of flow separation in three and four dimensions, 45th AIAA Aerospace Sciences Meeting and Exhibit, 8–11 Jan. 2007, Reno, NV, American Institute of Aeronautics and Astronautics, Paper AIAA-2006-401, 20 p.
- [3] Neubauer, J., Zhang, Z., Miraghaie, R., Berry, D. A., Coherent structures of the near field flow in a self-oscillating physical model of the vocal folds, *Journal of Acoustical Society of America*, 121 (2007), 1 102–1 118.
- [4] Pickup, B. A., Thomson, S. L., Influence of asymmetric stiffness on the structural and aerodynamic response of synthetic vocal fold models. *Journal of Biomechanics* 42 (2009) 2 219–2 225.
- [5] Punčochářová-Požížková, P., Furst, J., Horáček, J., Kozel, K., Numerical solutions of unsteady flows with low inlet Mach numbers, *Mathematics and Computers in Simulation*, 80 (2010) 1 795–1 805.
- [6] Titze, I. R., *Principles of voice production*, Iowa City, IA: National Center for Voice and Speech 2000.
- [7] Vampola, T., Horáček, J., Švec, J., FE modeling of human vocal tract acoustics. Part I: Production of Czech vowels, *Acta Acustica united with Acustica* 94 (2008) 433–447.